Quantitative multi-parametric MRI in characterization of ovarian cystic masses

Esam M Hemat; Khaled M El-Gerby and Ahmed A Ismail.

Radiology department, Faculty of Medicine, Zagazig University, Egypt.
esamhemat@yahoo.com

Abstract: Purpose: To assess quantitative multi-parametric MRI examination in characterization of ovarian complex cystic masses. **Patients:** Thirty female patients with a mean age of 47 years (31 to 64 years old) were presented with ovarian cystic masses by pelvic ultrasound or pelvic CT scanning. All patients were referred to radiology department for a pre-operative multi-parametric pelvic MRI. **Methods:** Conventional MRI, dynamic contrast enhanced MRI (DCE-MRI), and diffusion weighted imaging (DWI) with apparent diffusion coefficient (ADC) value were performed by a 1.5 T MRI machine. Regions of interest (ROIs) were applied over the solid and cystic components of the masses. Post-operative histopathology was done to determine the nature of ovarian cystic masses. **Results:** Thirty female patients were included (11 malignant & 19 benign cases by histopathology). DCE-MRI sequences had a significant higher mean values in malignant lesions than benign ones (*p-value* <0. 001). Regarding malignant lesions, time of initial peak of contrast uptake ranged from 55 to 100 seconds with an average 77 seconds. On the other side, benign lesions showed time of peak range from 58 to 230 seconds with an average of 104 seconds. The mean ADC value of benign lesions was ($1.36 \times 10^{-3} \pm 0.77$ mm^2/s), and of malignant lesions was ($0.58 \times 10^{-3} \pm 0.21$ mm^2/s). Our cutoff value was 1.23×10^{-3} mm^2/s. **Conclusion:** Multi-parametric MRI, such as conventional MRI criteria, DCE-MRI curves, diffusion weighted imaging (DWI) and apparent diffusion coefficient (ADC) value can independently differentiate benign from malignant ovarian masses.
[Esam M Hemat, Khaled M El-Gerby, and Ahmed A Ismail. **Quantitative multi-parametric MRI in characterization of ovarian cystic masses.** *J Am Sci* 2017;13(1):93-103]. ISSN 1545-1003 (print); ISSN 2375-7264 (online). http://www.jofamericanscience.org. 13. doi:10.7537/marsjas130117.13.

Key Words: Ovarian masses; dynamic contrast-enhanced MRI; quantitative MRI.

1. Introduction

Ovarian carcinoma is a main cause of women death from gynecological cancers in USA[1]. Ninety percent five-years survival in stage-I patients, but it significantly decrease to 40% in stage III and 30% in stage IV patients [2]. The survival rate of ovarian carcinoma is high for localized disease (up to 93%) and decreases significantly for regional and distant dissemination (up to 60% and 42%, respectively) [3].

The management outcome of patients with different ovarian lesions can significantly be improved by using new imaging modalities. New imaging modalities can screen and select patients referred to gynecologic oncologists of females who are at high risk for malignancy, this led to increase survival rates compared to surgical care only[4,5]. Many imaging diagnostic tools, such as ultrasonography (US), computed tomography (CT), and magnetic resonance imaging (MRI) have been investigated as screening and diagnostic methods, but to date none of them have demonstrated sufficient accuracy to predict malignancy either alone or together as a part of screening system[6-12]. Contrast-enhanced MRI has about 84-93% accuracy in detection of ovarian malignancy [13-16]. However, interpretation of these images is subjective and may vary depending on the reader experience [14]. There are a number of parameters that can be measured with MRI, including permeability and perfusion parameters derived from dynamic contrast enhanced MRI, relaxation rates, and diffusion-related parameters. Several of these parameters have been found to be associated with ovarian malignancy. Generally, malignant tumors have been shown to have shorter T2 values [17], increased perfusion based on dynamic contrast enhanced MRI parameters[18,19], and lower apparent diffusion coefficients (ADC) than that of benign tumors[20-22].

The aim of our study was to assess multi-parametric MRI in characterization of ovarian cystic masses (benign or malignant).

2. Patients and Methods

Patient characteristics:

This is a prospective study that was compliant with our institution committee ethics and a written consent was taken from all patients. Thirty women with a mean age of 47 years (ranged from 31 to 64 years), were presented with an ovarian cystic masses (based on pelvic US or pelvic CT scanning), were examined by conventional MRI, dynamic contrast enhanced MRI & DWI with ADC mapping. MRI scan was performed using a 1.5 Tesla superconducting MR machine (Philips–Achieva– Netherland), at radiology department of Zagazig University hospitals from November 2012 to November 2015.

MR Imaging protocol:

Non contrast conventional MRI

Axial T1-weighted FSE (TR/TE, 500/10 ms) **& Axial T2-weighted FSE** (TR/TE, 3300/100 ms). With slice thickness 6 mm Gap 1 mm. FOV 32–42 cm. Matrix 256 x 256.

Sagittal T2-weighted FSE & coronal T2-weighted FSE

Slice thickness 8-10mm. Gap 1 mm. FOV 40–50 cm. Matrix 256 x 256.

MR imaging analysis:

Conventional MRI evaluated for the following:

- MR morphology of the lesion; either cystic, solid or mixed.
- Lesion size & signal intensity.
- Pattern of enhancement, if present.
- Wall thickness, lesion regularity and its enhancement.
- Presence of vegetations and septations, their enhancement pattern and their size.
- Presence of intra-peritoneal fluid (ascites).
- Presence of infiltrated pelvic or para-aortic lymph nodes.
- Involvement of other pelvic organs.
- Presence of peritoneal and omental deposits.

☒ **MRI Signal characteristics for benign lesions:**

- Cystic lesions show low intensity in T1W images and high intensity on T2W images.
- Complex benign looking lesions: hyperintense signal on T1WI is considered either fat or blood. On fat suppressed images, drop of signal was noted with fat while hyperintense signal was still noted with blood.
- Solid lesions with very low signal intensity in T2WI are characteristic of fibrous tumor (e.g. ovarian fibroma).

☒ **Malignant MRI criteria:**

- Presence of wall thickness more than 3mm.
- Solid vegetations more than 10 mm.
- Thick septa more than 3mm.
- Areas of necrosis and breaking down.
- Signs of tumor spread for staging: enlarged lymph nodes, intra-peritoneal fluid, peritoneal and omental deposit.

Diffusion weighted magnetic resonance imaging analysis:

- **DWI** was achieved in the axial plane prior to administration of contrast medium by using a single shot echo-planar imaging sequence.
- With b values (0 &1000). TR/TE, 5000/70. Slice thickness 6 mm, Gap 1 mm, FOV 36 cm, Matrix 128 x128.

☒ **Interpretation of DWI:**

✓ **Qualitative analysis:**

Regarding the signal intensity: benign lesions were hypointense with a high signal in the corresponding ADC maps (facilitated diffusion), while malignant lesions were hyperintense with a low signal in the ADC maps (restricted diffusion).

✓ **Quantitative analysis:**

Regarding DWI, we generated the ADC map, and then we selected the ROI manually on the solid and the cystic component of the lesions, which was then automatically calculated on the workstation to get the mean ADC values.

DCE-MR images were obtained immediately after manually injection of gadolinium, 0.1 mmol/kg of body weight (maximum, 20 ml), followed by injection of 20 ml normal saline flush. Scans were taken in 0,30,60,90 and 120 sec from injection, sequentially. Finally, axial, sagittal and coronal T1W images were acquired.

Analysis:

Qualitative analysis of DCE-MRI:

Analysis of dynamic data were accomplished at a workstation. The entire ovarian lesion was included in all dynamic run acquisitions at (0, 30, 60, 90, and 120 second) after gadolinium injection. A region of interest (ROI) was drawn at the most enhancing area, thick enhanced wall and non enhanced wall of the lesion as well as at the myometrium and signal intensity (SI)–time curve was performed.

Quantitative analysis of DCE- MRI:

Maximum enhancement and time to peak were reported to know if there was early uptake (within the first 60 seconds) or not, and if maximum relative enhancement was more than 85% (with malignancy) or less.

Statistics:

Comparison of numerical variables between the study groups was done using Student *t* test for independent samples. Accuracy was determined by calculating sensitivity, specificity, positive predictive value, negative predictive value. Receiver operator characteristic (ROC) analysis was used to determine the optimum cut off value for the studied diagnostic markers. *P* values <0.05 was considered statistically significant. All statistical calculations were done using computer programs SPSS (Statistical Package for the Social Science; SPSS Inc., Chicago, IL, USA) version 15 for Microsoft Windows.

All data analysis of conventional MRI, DCE-MRI & DWI with ADC map were correlated with surgery and histopathology.

3. Results

Thirty women patients with ovarian cystic masses were included in the study. All patients were prepared for ovarian cystic masses excision. Nineteen patients with benign ovarian masses (Figures1,2,4)

and 11 patients with malignant ovarian masses (Figure 3). Patients age, Ca-125 level, cystic ROIs, solid ROIs, ADC values and histopathological diagnosis of benign and malignant cases were detailed in tables 1&2 respectively.

Table (1): Age, Ca-125, cystic ROIs, solid ROIs, mean ADC values and pathological types of benign cases.

Patient No	Mean age	Mean Ca125	Cystic ROIs	Solid ROIs	Mean ADC value ±SD	Histo-pathological diagnosis
2	33	15	4	-	$1.42x10^{-3} \pm 0.77$ SD mm^2/s	Hemorrhagic cysts
1	44	10	1	-	$1.70x10^{-3} \pm 0.78$ SD mm^2/s	Simple cyst
1	43	14	2	-	$1.29x10^{-3} \pm 0.67$ SD mm^2/s	Dermoid cyst
2	34	18	3	-	$0.92x10^{-3} \pm 0.37$ SD mm^2/s	Endometriosis
1	40	-	3	1	$0.67x10^{-3} \pm 0.55$ SD mm^2/s	Tubo-ovarian abscess
1	38	22	2	1	$0.69x10^{-3} \pm 0.42$ SD mm^2/s	Mature teratoma
1	37	48	3	1	$1.37x10^{-3} \pm 0.77$ SD mm^2/s	Fibroadenoma
1	52	8	1	1	$1.37x10^{-3} \pm 0.77$ SD mm^2/s	Brenner tumor
4	48	15	9	-	$1.39x10^{-3} \pm 0.77$ SD mm^2/s	Serous cyst-adenomas
5	50	38	15	1	$1.40x10^{-3} \pm 0.77$ SD mm^2/s	Mucinous cyst-adenomas

Table (2): Age, Ca-125, cystic ROIs, solid ROIs, mean ADC values and pathological types of malignant cases.

Patient No	Mean age	Mean Ca125	Cystic ROIs	Solid ROIs	Mean ADC value ±SD	Histo-pathological diagnosis
1	51	800	1	1	$0.63x10^{-3} \pm 0.27$ SD mm^2/s	Fibrosarcoma
1	48	700	1	1	$0.56x10^{-3} \pm 0.21$ SD mm^2/s	Endometroid adenocarcinoma
1	50	195	2	1	$0.57x10^{-3} \pm 0.21$ SD mm^2/s	clear cell carcinoma
2	52	190	7	4	$0.58x10^{-3} \pm 0.21$ SD mm^2/s	Mucinous adenocarcinomas
6	55	340	21	14	$0.56x10^{-3} \pm 0.21$ SD mm^2/s	Serous cystadenocarcinomas

We prescribed 101 lesion ROIs in all patients. Cystic ROIs were more common than solid ROIs (75 cystic ROIs and 26 solid ROIs); 19 benign cases showed 5 solid and 43 cystic ROIs, whereas, 11 malignant cases showed 21 solid and 32 cystic ROIs (Tables 1,2). In table (1) the common benign lesions were mucinous cystadenoma (5 cases) and serous cystadenoma (4 cases), however, the most common malignant lesion was serous cystadenocarcinoma (6 cases) (Table 2).

The dimensions of benign lesions ranged from 2.8 to 12 cm (mean dimension was 6.45 ± 3.06) and malignant lesions dimensions ranged from 5.5 to 18 cm (mean dimension was 10.55 ± 2.89 as shown in table (3).

Table (3): Represents the various diameters of the lesions:

Dimension	Benign lesions	Malignant lesions
Minimum	2.8 cm	5.5cm
Maximum	12 cm	18cm
Mean	6.45 ± 3.06	10.55 ± 2.89

The mean ADC value for benign lesions was ($1.36 \times 10^{-3} \pm 0.77$ mm^2/s), and for malignant lesions was ($0.58x\ 10^{-3} \pm 0.21$ mm^2/s) (table 4). The cutoff value of our results was 1.23×10^{-3} mm^2/s.

Table (4): Minimum, maximum ± SD and mean ADC values in benign and malignant ovarian lesions.

	No of patients	Minimum	Maximum	Std. deviation	Mean
Benign	19	$0.5x10^{-3}$ mm^2/s	$2.6x10^{-3}$ mm^2/s	± 0.77	$1.36x10^{-3}$ mm^2/s
Malignant	11	$0.3x10^{-3}$ mm^2/s	$0.9x10^{-3}$ mm^2/s	± 0.21	$0.58x10^{-3}$ mm^2/s

t. test = 8.770 *p. value* = 0.007

Three borderline cases (one tubo-ovarian abscess, one endometrioma and one mature cystic teratoma) were included in our study, and were revealed a heterogeneous intermediate to high signal intensity on DWI with low ADC values (0.6, 0.9 and 0.6×10^{-3} mm^2/s), respectively.

Three types of enhancement curves were resulted from DCE-MRI study. Seventeen cases revealed enhancement pattern in the form of slow rising curve (gradual enhancement with no definite peak), that confirmed a benignity of those lesions. Ten cases showed enhancement pattern of rapid steep rising curve (early enhancement of solid portions and delayed washout), that confirmed malignant nature of those lesions.

Our results showed that most DCE-MRI sequences had a significant higher mean values in malignant lesions than benign lesions (p-value<0. 001).

Regarding malignant lesions, time of initial peak of contrast uptake ranged from 55 to 100 seconds with an average 77 seconds. On the other side, benign lesions showed time of peak range from 58 to 230 seconds with an average of 104 seconds.

The three borderline cases (tubo-ovarian abscess, endometriosis and mature cystic teratoma) showed an initial enhancement followed by plateau curve in DCE-MRI.

The total sensitivity, specificity, PPV, NPV, over all accuracy and p-value of conventional MRI, DCE-MRI and DWI in characterization of ovarian cystic masses (detection of their malignancy), compared with histopathology, were summarized in table (5).

Table (5) showed that DCE-MRI and DWI were more specific, sensitive and more accurate than conventional MRI alone.

Table (5): Sensitivity, specificity, PPV, NPV, over all accuracy & *p.*value of conventional MRI, DCE-MRI and DWI in characterization of ovarian masses compared with histopathology.

	Conv. MRI	DCE-MRI	DWI-MR
Sensitivity	86%	88.9%	100%
Specificity	82%	87%	87%
PPV	73%	80%	82%
NPV	92%	100%	100%
Accuracy	84%	87.8%	92%
P. value	0.625	0.911	0.016

PPV (Positive predictive value). *NPV (Negative predictive value).*

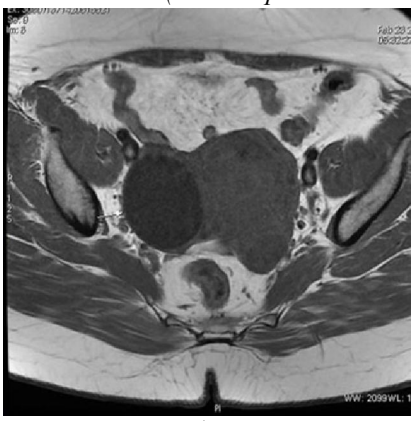

A

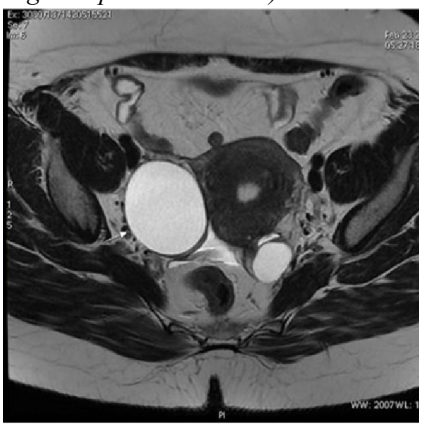

B

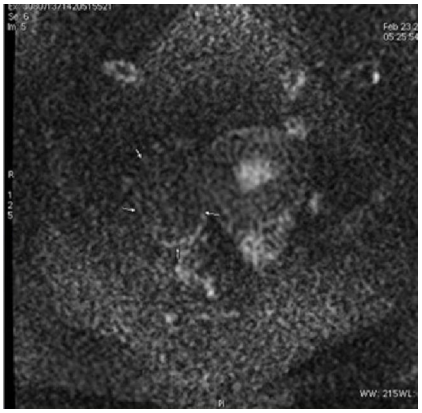

C

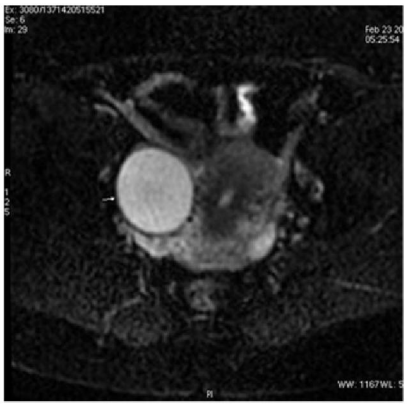

D

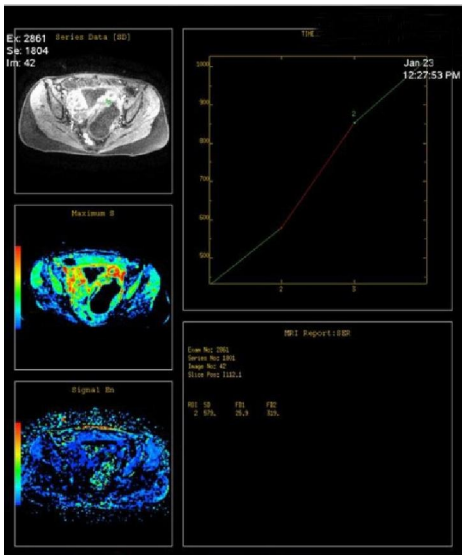

E

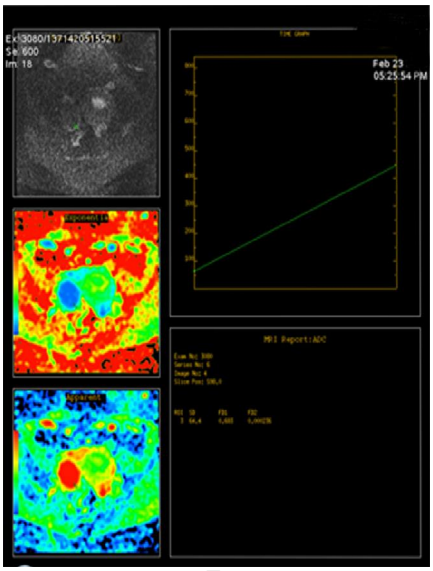

F

Figure-1(A-F): Simple right adenxal cvst in a 44 year-old women (a) Unenhanced T1-weighted axial image.(b) T2-weighted axial image show a cyst at right ovary demonstrates clear fluid signal intensity.(c) Diffusion-weighted (b=1000 sec/mm2) show that, the cyst demonstrate hypointense signal (arrows) (d) Corresponding ADC map shows that the cyst demonstrates high signal intensity with high ADC value= $1.7x10^{-3}$ cm/s). (e,f) Graphs show the dynamic enhanced time-intensity curve for the selected ROI during the three-point dynamic run, shows slower and less intense enhancement than the myometrium suggesting benignity.

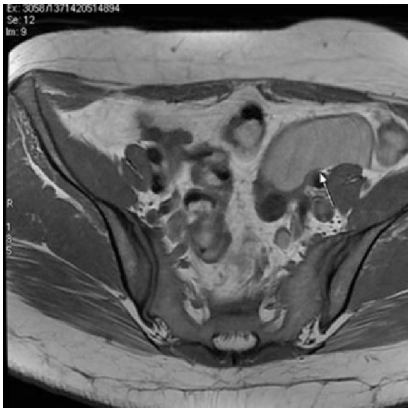

A

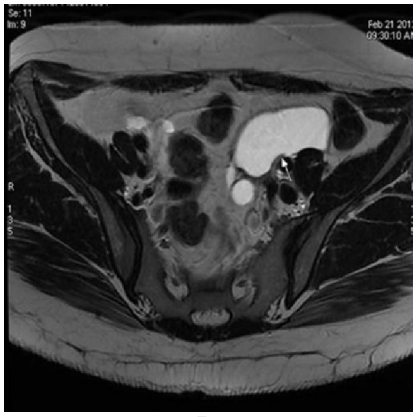

B

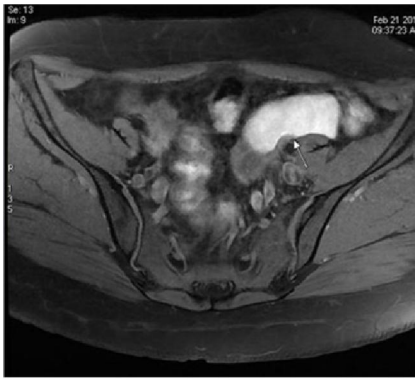

C

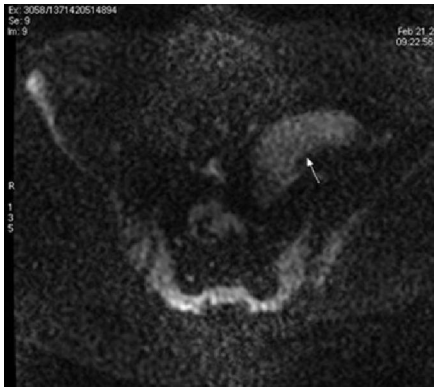

D

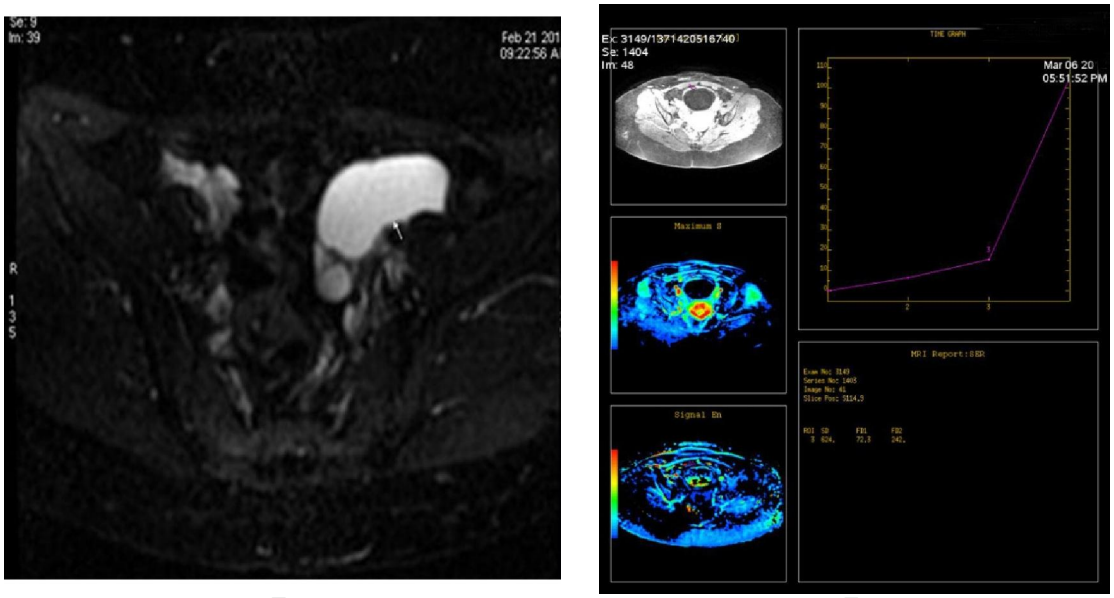

E F

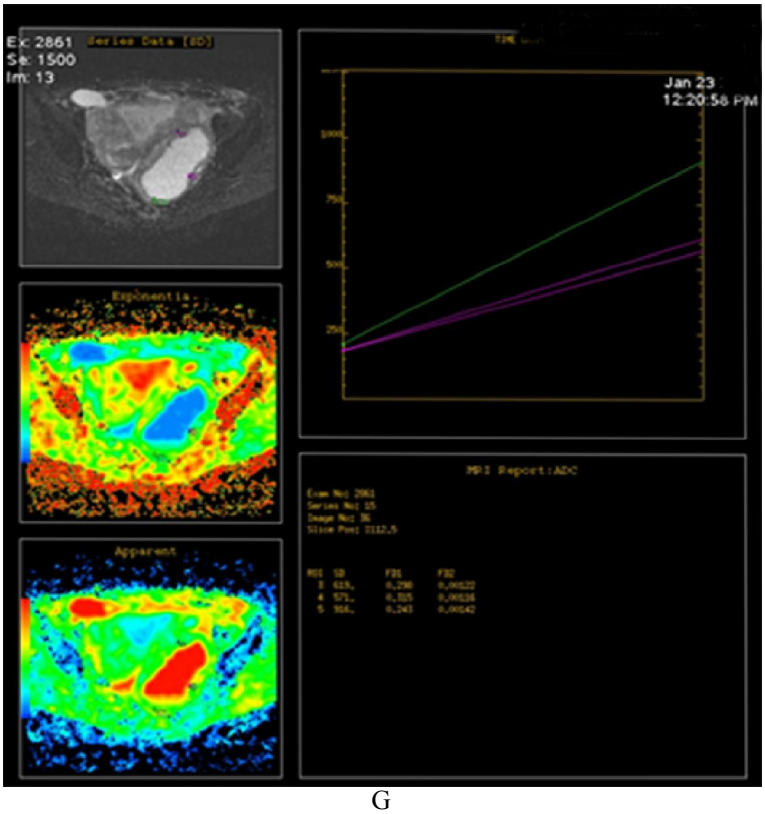

G

Figure-2(A-G): Complex haemorrhagic bilateral adenxal cysts in a 40 year-old woman (a) Unenhanced T1-weighted axial image. (b) T2-weighted axial image. (c) FAT-SAT T1-weight axial image show well circumscribed adenxal cysts at right and left ovaries, the left one shows predominantly hyperintense signal anteriorly, a findings suggesting blood which confirmed by non drop of signal at FAT-SAT image, and an area of low signal posteriorly as well as at right ovary and may represent debris, blood and serous fluid, (d) Diffusion-weighted (b=1000 sec/mm2) show low signal intensity. (e) Corresponding ADC map shows high signal intensity, suggesting a benign cysts. (f,g) graphs show dynamic enhanced curves.

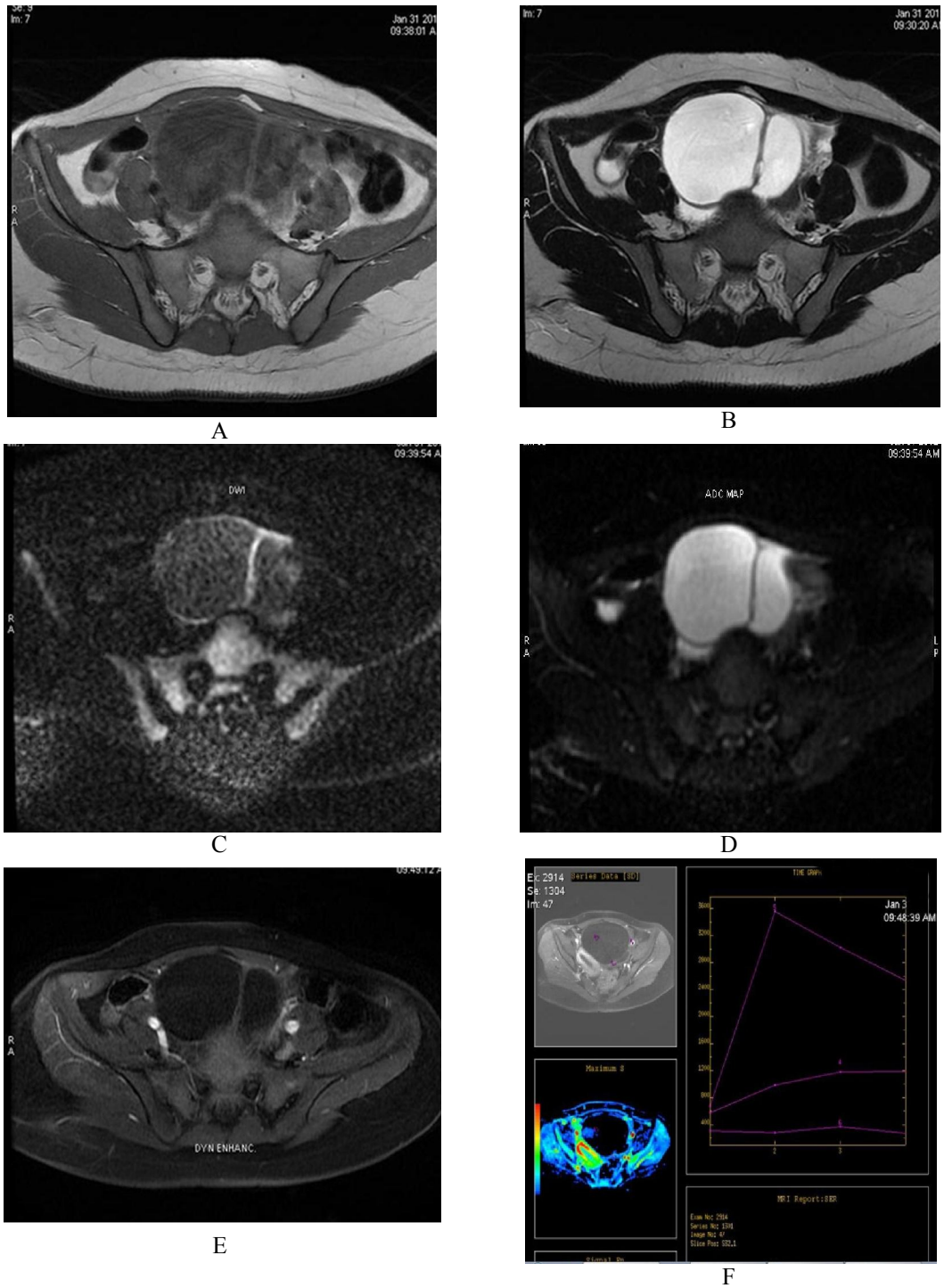

Figure-3(A-G): Malignant high grade serous carcinoma in a 52 year-old postmenopausal woman (a&b) Axial T1 and T2-weighted images show bilocular adenxial cyst at left ovary with fluid signal intensity with irregular septum (c) Axial T1-weighted fat-suppressed dynamic image, obtained at 0 seconds post-contrast shows intense early peripheral and septal enhancement. ROIs are drawn over enhancing areas and adjacent myometrium (d) Graph shows the dynamic contrast-enhanced time-intensity curves, which indicate that wall and septum demonstrate greater and more, rapid early enhancement than myometrium (e) Diffusion-weighted (b=1000 sec/mm2) shows that enhanced periphery and septum demonstrates restricted diffusion with high signal intensity (arrows).(f,g) Corresponding ADC map shows that enhanced areas demonstrate low signal intensity. These criteria highly suggest malignancy.

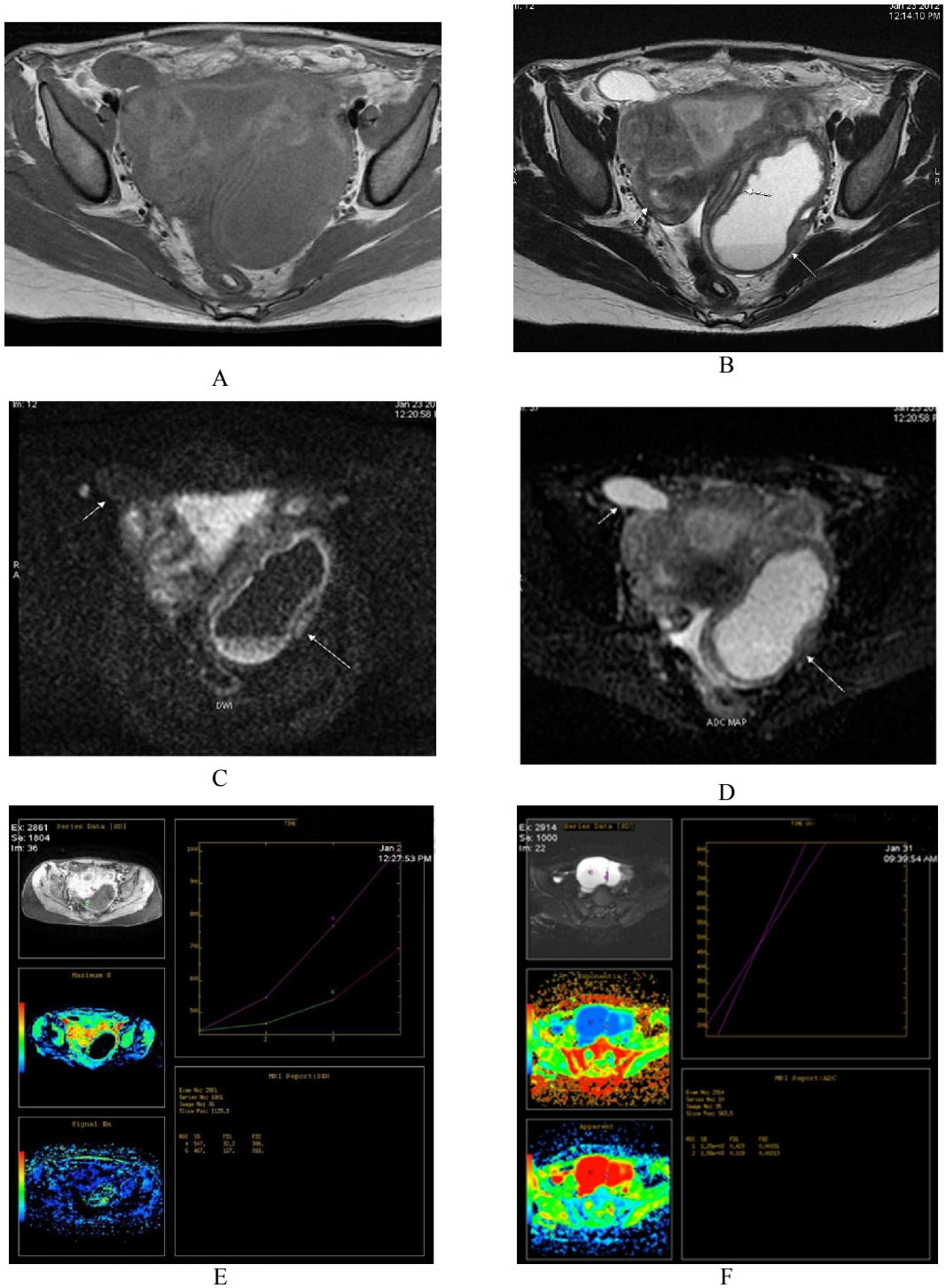

Figure-4(A-F): Bilateral tubo-ovarian TB (a,b) Axial T1 and T2-WI show bilateral cystic masses (c) Axial T1-W fat-suppressed enhanced image show partial enhancement (d) (f) ADC map show low signal.(e,f) Dynamic curves demonstrate slow enhancement anf display high signal

4. Discussion

Ovarian carcinoma is the second gynecological cancer and the fifth common carcinoma in adult females [23]. Unfortunately, most patients were discovered late, and had a poor survival rates. Proper and early diagnosis of ovarian cancer can help in finding more available treatment options and lead to better prognosis [24]. Nowadays, most clinicians prefer

a noninvasive staging to decide a neo-adjuvant chemotherapy, if indicated, that permits downstaging before a surgical intervention [25].

In the present work, feasibility of applying multi-parametric MRI for characterization of ovarian cystic masses was demonstrated, and we found many parameters based on DCE-MRI, diffusion imaging, and apparent diffusion coefficient values that were significantly associated with malignancy. Purely cystic ovarian masses are more likely to be benign.

Conventional MRI can assess morphologic criteria of the lesion, such as wall thickening, intra-luminal papilla, nodules, thick septa and signal intensity on T1W and T2W images, but none of these criteria reliably can differentiate benign from malignant lesions [26].

Development of a new MRI parameters to improve the diagnostic technology, screening of high risk patients and treatment monitoring motivates the investigation into functional and multi-parametric MRI [17].

Diffusion weighted imaging is one of the promising functional imaging techniques, and it is able to differentiate ovarian masses; benign or malignant [27].

DCE-MRI findings show early intense enhancement of malignant masses, consistent with many previous literatures [19-21], as ovarian malignant lesions have a high vascularity, compared with benign lesions.

We had performed an individual analysis for conventional MRI, DCE-MR imaging and DWI with ADC map, regarding their diagnostic performance in the characterization of different cystic ovarian masses.

We found that the sensitivity of conventional MRI on individual basis was slightly lower than DCE-MRI. The specificity was higher for DCE (87%) compared to pre-contrast MRI sequences (82%), as well as the PPV, NPV and accuracy were higher for DCE-MRI (80%, 100% & 87.87% respectively), while that of conventional MRI were (73%, 92% & 84% respectively), so addition of DCE to the MRI was expected to increase the specificity and the accuracy of examination.

Sohaib *et al.,* [16] and Nasr *et al.,*[31] stated that malignant lesions show more intense enhancement than benign lesions during the early phase of post-contrast enhancement, rather than the late phase of enhancement, whereas benign tumors show slower sustained lower enhancement.

In our results, DWI had shown 100% sensitivity in its individual performance during the assessment of the included ovarian lesions, the specificity was (87%), PPV was (82%), NPV was (100%) & accuracy was (92%), while conventional MRI showed a sensitivity (86%), specificity (82%), PPV (73%), NPV (92%) and accuracy (84%).

In the quantitative assessment, the mean ADC values for malignant lesions was ($0.58x\ 10^{-3} \pm 0.21$ mm^2/s), and for benign lesions was ($1.36 \times 10^{-3} \pm 0.77 mm^2/s$). Our cutoff value was 1.23×10^{-3} mm^2/s.

Fujii *et al.,* [28] & Kierans, *et al.,* [29] showed that most malignant ovarian tumors as well as some of the cystic mature teratomas and endometriomas showed high signal intensity on DWI, whereas, most of the benign lesions did not. This agree with our results, whereas, all malignant lesions (11cases) and one case of mature cystic teratoma & one case endometrioma showed a high signal on DWI, this may be attributed to keratinized substance in mature cystic teratoma, and intra-cystic blood clots in endometrioma.

In 2009, Thomassin *et al.,*[21] evaluated contribution of DWI in conjunction with morphological criteria to characterize 77 complex ovarian masses (30 benign and 47 malignant). According to them, low signal intensity on T2-weighted images with loss of restricted diffusion signal in solid region of mixed adnexal masses may predict benignity.

A similar study was carried out by Takeuchi *et al.,* [30] and Nasr *et al.,*[31] who stated that the solid portions of a malignant masses showed homogenous or heterogeneous high signal intensity on DWI. The mean ADC value in malignant tumors was 1.03×10^{-3} mm^2/s, however, in benign tumors was 1.38×10^{-3} mm^2/s. Consequently, they concluded that low DWI signal intensity and high ADC value may suggest benignity.

In the study of Li *et al.,*[24] and Kierans, *et al.,* [29] the mean ADC value measured for the ovarian cystic region did not distinguish between benign and malignant lesions significantly. Unlike that measured for the solid region which significantly differentiate benign from malignant lesions. Mean ADC value for benign masses was $1.69 \times 10^{-3} \pm 0.25$ mm^2/s, and for the malignant masses was $1.03 \times 10^{-3} \pm 0.22$ mm^2/s. Their results suggested that an ADC value $\geq 1.25 \times 10^{-3}$ mm^2/s may be an optimal cut-off value in differentiation between benign and malignant ovarian lesions.

Also, Zhang *et al.,*[28], found that DWI is a useful parameter for differentiation between benign ovarian tumors with solid components and malignant ovarian tumors, with a high sensitivity and specificity.

Zhao *et al.,*[33] and Musto *et al.,* [34] found that the majority of malignant ovarian epithelial tumors were hyperintense on DWI, whereas most borderline epithelial ovarian tumors were hypointense or moderately intense. Mean ADC value of the solid component of borderline epithelial ovarian tumor ($1.562\pm\ 0.346 \times 10^{-3}$ mm^2/s) was higher than

malignant epithelial ovarian tumor (0.841 ± 0.209 x 10^{-3} mm^2/s).

Our study included 3 borderline lesions (one tubo-ovarian abscess, one endometrioma and one mature cystic teratoma) of low malignant potential. These lesions showed a heterogeneous intermediate to high signal intensity on DWI and low ADC values of 0.6, 0.9 & 0.6 x 10^{-3} mm^2/s respectively.

Conclusion: Multi-parametric quantitative MRI, increase the sensitivity, the specificity and over all accuracy for characterization of cystic ovarian masses and help in differentiating benign from malignant ovarian masses. So, we recommend the addition of DCE-MRI and DWI with ADC mapping to conventional MRI in assessment of ovarian cystic masses for accurate diagnosis and better management.

References

1. Ahmedin J, Rebecca S, Ward E, Hao YJ, Jiaquan Xu, Michael J. American, Cancer Society. Cancer Facts and Figures 2009. Atlanta: American Cancer Society, 2009; Volume 59, Issue 4: 225-249.
2. Munkarah A, Chatterjee M, Tainsky M. Update on ovarian cancer screening. Curr Opin Obstet Gynecol 2007; 19:22-26.
3. Bagade S, Fowler KJ, Schwarz J K, Grigsby PW, and Dehdashti F. PET/MRI Evaluation of Gynecologic Malignancies and Prostate Cancer. Semin Nucl Med 2015; 45:293-303.
4. Earle CC, Schrag D, Neville BA, Yabroff KR, Topor M, Fahey A, *et al.* Effect of surgeon specialty on processes of care and outcomes for ovarian cancer patients. J Natl Cancer Inst 2006; 98(3):172-180.
5. Mercado C, Zingmond D, Beth Y. Karlan, Sekaris D, Gross J, Maggard-Gibbons M, *et al.* Quality of care in advanced ovarian cancer: the importance of provider specialty. Gynecol Oncol 2010; 117(1): 18-22.
6. Usha Menon, Aleksandra Gentry-Maharaj, Rachel Hallett, Andy Ryan, Matthew Burnell, Aarti Sharma, *et al.* Sensitivity and specificity of multimodal and ultrasound screening for ovarian cancer, and stage distribution of detected cancers: results of the prevalence screen of the UK Collaborative Trial of Ovarian Cancer Screening (UKCTOCS). Lancet Oncol 2009;10(4):327-340.
7. Buy J N, Ghossain M A, Hugol D, Hassen K, Sciot C, Truc J B, *et al.* Characterization of ovarian masses: combination of color Doppler and conventional sonography compared with spectral Doppler analysis alone and conventional sonography alone. AJR 1996;166:385-393.
8. Stein SM, Laifer-Narin S, Johnson MB, Roman LD, Muderspach LI, Tyszka JM, *et al.* Differentiation of benign and malignant adnexal masses: relative value of gray-scale color Doppler and spectral Doppler sonography. AJR 1995;164(2):381-386.
9. Levine D, Felstein VA, Babcock CJ, and Filly AR. Sonography of ovarian masses: poor sensitivity of resistive index for identifying malignant lesions. AJR 1994;162:1355-1359.
10. Rehn M, Lohmann K, and Rempen A. Transvaginal ultrasonography of pelvic masses: evaluation of B-mode technique and Doppler ultrasonography. Am j Obstet Gynecol 1996; 175(1):97-104.
11. Buys SS, Partridge E, Greene MH, Prorok PC, Reding D, Riley TL, *et al.* PLCO Project Team. Ovarian cancer screening in the Prostate, Lung, Colorectal and Ovarian (PLCO) cancer screening trial; findings from the initial screen of a randomized trial. Am J Obstet Gynecol. 2005; 193(5):1630-1639.
12. Buys SS, Partridge E, Black A, Johnson CC, Lamerato L, Isaacs C, *et al.* PLCO Project Team. Effect of screening on ovarian cancer mortality: the prostate, lung, colorectal and ovarian (PLCO) cancer screening randomized controlled trial. JAMA 2011;305(22):2295-2303.
13. van Nagell JR, DePriest PD, Ueland FR, DeSimone CP, Cooper AL, McDonald JM, *et al.* Ovarian cancer screening with annual transvaginal sonography: findings of 25.000 women screened. Cancer 2007; 109(9):1887-1896.
14. Booth SJ, Turnbull LW, Poole DR, and Richmond I. The accurate staging of cancer using 3T magnetic resonance imaging–a realistic option. BJOG 2008;115:894-901.
15. Hircak H, Chen M, Coakley FV, Kinkel K, Yu KK, Sica G, *et al.* Complex adnexal masses: detection and characterization with MR imaging-multivariate analysis. Radiology 2000; 214:39-46.
16. Sohaib SA, Sahdev A, Van Trappen P, Jacobs IJ, and Reznek RH. Characterization of adnexal mass lesions on MR imaging. Am J Roentgenol. 2003 Vols. 180(5): 1297-1304.
17. Thomassin-Naggara I, Toussaint I, Perrot N, Rouzier R, Cuenod CA, Bazot M, *et al.* Characterization of complex adnexal masses: value of adding perfusion-and diffusion-weighted MR imaging to conventional MR imaging. Radiology 2011; 258(3):793-803.
18. Thomassin-Naggara I, Darai E, Cuenod CA, Rouzier R, Callard P, and Bazot M. Dynamic contrast-enhanced magnetic resonance imaging:

a useful tool for characterizing ovarian epithelial tumors. J Magn Reson Imaging 2008; 28:111-120.
19. Thomassin-Naggara I, Bazot M, Darai E, Callard P, Thomassin J, and Cuenod CA. Epithelial ovarian tumors: value of dynamic contrast-enhanced MR imaging and correlation with tumor angiogenesis. Radiology 2008; 248(1): 148-159.
20. Moteki T, and Ishizaka H. Diffusion-weighted EPI of cystic ovarian lesions: evaluation of cystic contents using apparent diffusion coefficients. J Magn Reson Imaging 2000: 12(6): 1014-1019.
21. Thomassin-Naggara I, Darai E, Cuenod CA, Rouzier R, Callard P, and Bazot M. Contribution of diffusion-weighted MR imaging for predicting benignity of complex adnexal masses. Eur Radiol. 2009; 19: 1544-1552.
22. Le Bihan D, Breton E, Lallemand D, Eubin ML, Vignaud J, Laval-Jeantet M. Separation of diffusion and perfusion in intravoxel incoherent motion MR imaging. Radiology 1998;168;(2):497-505.
23. Wenhua Li, Caiting Chu, Yanfen Cui, Ping Zhang, and Minjie Zhu. Diffusion- weighted MRI: a useful technique to discriminate benign versus malignant ovarian surface epithelial tumors with solid and cystic components. Abdom Imaging 2012; 37;(5): 897–903.
24. Reynolds E and Moller K. A review and an update on the screening of epithelial ovarian cancer. Curr Probl Cancer 2006; 30:203-232.
25. Schmidt S, Meuli RA, Achtari C, and Prior JO. Peritoneal Carcinomatosis in Primary Ovarian Cancer Staging Comparison Between MDCT, MRI, and 18 F-FDG PET/CT. Clin Nucl Med 2015;40: 371–377.
26. Valentini AL, Micco BG, Mingote MC, De Gaetano AM, Ninivaggi V, and Bonomo L. Benign and Suspicious Ovarian Masses—MR Imaging Criteria for Characterization: Pictorial Review, Journal of Oncology, 2012;15: 1-9.
27. Parker GJ, Roberts C, Macdonald A. Buonaccorsi GA, Cheung S, Buckley DL, et al. Experimentally derived functional form for a population –averaged high-temporal-resolution arterial input function for dynamic contrast-enhanced MRI. Magn Reson Med 2006;56(5): 993-1000.
28. Fujii, S.; Kakite, S. and Nishihara, K. Diagnostic accuracy of diffusion weighted imaging in differentiating benign from malignant ovarian lesions. J. Magn. Reson. Imaging 2008; 28:1149-1156.
29. Kierans AS, Bennett GL, Mussi TC, Babb JS, Rusinek H, Melamed J, and Rosenkrantz AB. Characterization of Malignancy of Adnexal Lesions Using ADC Entropy: Comparison With Mean ADC and Qualitative DWI Assessment. J. Magn. Reson. Imaging 2013;37:164–171.
30. Takeuchi M, Matsuzaki K and Nishitani H. Diffusion-Weighted Magnetic Resonance Imaging of Ovarian Tumors: Differentiation of Benign and Malignant Solid Components of Ovarian Masses. J Comput Assist Tomogr 2010; 34: 173-176.
31. Nasr E, Hamed I, Abbas I and Khalifa NM. Dynamic contrast enhanced MRI in correlation with diffusion weighted (DWI) MR for characterization of ovarian masses. Egypt J Radiol Nucl Med (2014), p 1-11.
32. Zhang P, Cui P, Li W, Ren G, Chu C, and Wu X. Diagnostic accuracy of diffusion-weighted imaging with conventional MR imaging for differentiating complex solid and cystic ovarian tumors at 1.5T. World Journal of Surgical Oncology 2012,10:237.
33. Zhao SH, Qiang JW, Zhang GF, Wang SJ, Qui HY, and Wang L. MRI in differentiating ovarian borderline from benign mucinous cystadenoma: pathological correlation, J Magn Reson Imaging, 2014;39(1):162-6.
34. Musto A, Grassetto G, Marzola MC, Rampin L, Chondrogiannis S, Maffione AM, et al. Management of epithelial ovarian cancer from diagnosis to restaging: an overview of the role of imaging techniques with particular regard to the contribution of 18 F-FDG PET/CT. Nuclear Medicine Communications 2014, 35:588–597.

1/17/2017